RJC

RASĀYAN *J. Chem.*
Vol. 18 | No. 3 |1474-1481| July-September | 2025
ISSN: 0974-1496 | e-ISSN: 0976-0083 | CODEN: RJCABP
http://www.rasayanjournal.com
http://www.rasayanjournal.co.in

OPTIMIZATION AND MODELING OF DYE DEGRADATION BY CeO_2/Fe_2O_3/rGO NANOCOMPOSITE USING RESPONSE SURFACE METHODOLOGY

K. Satyam Naidu[1,2,✉], Nowduri Annapurna[2], R. S. K. Sharma[1] and G. V. Siva Prasad[1]

[1]Department of Chemistry, Raghu Engineering College (A), Visakhapatnam-531162, (AP), India
[2]Department of Engineering Chemistry, AU College of Engineering (A), (Andhra University), Visakhapatnam-530003, (AP), India
✉Corresponding author: satymnaidu.kandi@raghuenggcollege.in

ABSTRACT

The present study reports the in-situ synthesis of CeO_2/Fe_2O_3/r-GO (CFG) nanocomposites through the approach of co-precipitation. The Box–Behnken Design (BBD) of Response Surface Methodology (RSM) was applied to optimize the visible-light degradation of eosin blue and indigo carmine dyes. The material was characterized using XRD, UV-DRS, TEM, EDX, and XPS techniques. Four input variables, pH (4–12), catalyst dosage (25–75 mg/L), dye concentration (2–6 mg/L), and time of irradiation (30–120 minutes), were studied. Regression analysis showed good model fit with R^2 values of 0.9962 (eosin blue) and 0.9729 (indigo carmine). ANOVA confirmed model accuracy. Optimum conditions for maximum degradation were pH 8.7, 66.32 mg/L catalyst, 3.1 mg/L dye, and 120 min for indigo carmine, and pH 9.8, 64.5 mg/L catalyst, 3.9 mg/L dye, and 120 min for eosin blue. Predicted removal efficiencies were 88.31% and 86.22%, respectively, confirming CFG's effectiveness in dye degradation. This research supports Sustainable Development Goals 6 and 12, promoting advanced, sustainable technologies for water purification and responsible resource utilization.

Keywords: CeO_2/Fe_2O_3/r-GO, Photo Catalyst, Indigo Carmine, Eosin Blue, Response Surface Methodology, Box–Behnken Design.

RASĀYAN *J. Chem.*, Vol. 18, No. 3, 2025

INTRODUCTION

Color materials that are released into the environment can have adverse consequences.[1,2] More than ten thousand different types of chemical dyes are thought to exist. Each year, over 700,000 tons of dyes are produced globally, contributing significantly to industrial wastewater.[3] Almost 10% is lost during the production and processing of dye, and this 20% loss is absorbed by the industrial system, according to diverse study findings. Water quality is negatively impacted by the presence of color, which is visible at extremely low quantities (even less than 1 mg/L).[4-5] Discharging untreated wastewater or effluent into the surrounding environment might have negative effects on water-based life and photosynthesis by limiting light transmission.[6] The following are examples of health impacts on humans: cyanosis, allergy, skin irritation, dermatitis, vomiting, jaundice, shock, quadriplegia, mutations, tissue necrosis, cancer, and death.[7] dyes can be categorized according to their solubility and insolubility. Acidic, basic, metal, mordant, complex, direct, and reactive dyes are examples of soluble dyes. Among the insoluble dyes are dispersion, azoic, and sulfur.[8] Dyes can be divided into three categories in one direction: cationic, anionic, and non-ionic.[9] Anionic dyes have less toxicity than cationic dyes.[10] Indigo carmine dye is a cationic color. Eosin (EY) is an anionic dye belonging to the xanthene group. Although treating wastewater presents a number of difficulties and problems, contemporary methods should be simple, inexpensive, and environmentally benign.[11] Recent advancements in nanotechnology have demonstrated a number of benefits for water treatment, including low cost, high efficacy, and reusable nature.[12] Owing to the special qualities of nanomaterials, such as their vast surface area and low concentration requirement, they have enormous potential for treating contaminated water that contains various organic and inorganic pollutants, as well as metal toxins.[13] Because of their unique surface characteristics and quantum effects under light irradiation, the Photo-Nano catalysts responded differently to light than bulk materials did.[14] Multiple research projects

http://doi.org/10.31788/RJC.2025.1839317

have reported on the application of photo catalysis to treat wastewater using dissolved organic matter mineralization or breakdown.[15] Due to its exceptional optical and electrical qualities, semiconductor nanomaterials-based reduced graphene oxide has recently attracted a lot of attention. Its photocatalytic performance can be enhanced by employing a variety of techniques, including the template method, chemical doping, and physical composite systems.[16] Numerous studies have documented the synthesis of photocatalytic materials and their use in the organic contaminant degradation process by increasing the e-h pair separation efficiency.[17] All of these studies have used photo-catalyzed breakdown of organic molecules using light (UV, Visible, and Solar) mediated by semiconductors. Numerous papers have examined the process of photocatalytic remediation for organic contaminants.[18] Tackling these global issues directly supports SDG 6 (Clean Water and Sanitation), which focuses on reducing pollution and enhancing water quality. Eco-friendly materials and energy-efficient degradation methods promote sustainable industry operations, which coincide with SDG 12 (Responsible Consumption and Production). The present work is to create CeO_2/Fe_2O_3/r-GO(CFG) as inexpensive, easily prepared, and effective photoactive nanoparticles. A new technique has been developed. This work has explored the potential applications of these nanomaterials in the treatment of industrial wastewater that is contaminated. Statistical approaches are essential for experimental designs when there is a relationship between several factors and the process outcome. These techniques assist in choosing a suitable design to reduce the amount of materials used, the cost of the tests, and the amount of time needed for the experiments. In situations where multiple independent variables interact to influence the intended results, RSM becomes a valuable process optimization approach. RSM fits a model using the least squares method based on an experimental design such as BBD.[19] The study assesses the degradation efficiency of Indigo Carmine (IC) and Eosin Blue (EB) using the CFG nanocomposite. The analysis is supported by diagnostic tests through ANOVA, with the process optimization done via a statistical approach based on Response Surface Methodology (RSM), particularly employing the Box–Behnken Design (BBD). CFG nanocomposite demonstrates significant potential as a catalyst for degrading pollutants in aqueous streams, and the study examines the effects and interactions of various factors on the degradation process.

EXPERIMENTAL

Materials

All substances obtained were of analytical quality and were used without additional purification for dye degradation experiments. Graphite flakes, ferrous sulphate $FeSO_4.7H_2O$, cerium chloride $CeCl_3.7H_2O$, and urea were acquired from Sigma-Aldrich.

Preparation of the CFG Nanocomposite

A 1:1 stoichiometric ratio of $CeCl_3.7H_2O$ and $FeSO_4.7H_2O$ was dissolved in 50 mL of DD water. After that, 0.1 g of the as-synthesized GO was introduced into the mixture along with a 0.1 M urea (CH_4N_2O) solution. For half an hour, the mixture was continually mixed while being ultrasonically sonicated for 30 minutes. The combination spent eighteen hours at 180°C after being moved to a 100 mL autoclave. CFG nanocomposite was obtained by collecting the precipitate, washing it with DI water and ethanol, drying it in an oven, and then calcining it for two hours at 400°C.[20]

Box Behnken Design (BBD) within the Response Surface Approach:

In order to maximize the degradation efficiency of the dye, the BBD was utilized in this procedure. This model consists of three levels: high, medium, and low, represented with the codes +1, 0, and -1. There were 27 trial runs carried out repeatedly to optimize the selected variables: pH of solution (X_1), Dosage of catalyst (X_2), dye concentration (X_3), and time of irradiation (X_4). The range and levels (coded and actual) of the independent or process variables used in this study are summed up in Table-1. The interrelationship among the four independent variables and the % degradation is represented by the quadratic Eqn.-1.[19]

$$Y = \beta_0 + \sum_{i=1}^{n} \beta_i X_i + \sum_{i=1}^{n} \beta_{ii} X_i^2 + \sum_{1 \le i \le j}^{n} \beta_{ij} X_i X_j + \varepsilon \quad (1)$$

Where,

Y refers to the estimated response, expressed as the percentage of degradation.

β_0 represents the intercept or baseline value in the model.

β_i signifies the contribution of the linear term for each independent variable.
β_{ii} corresponds to the squared (quadratic) influence of a given variable.
β_{ij} captures the interaction effect between the two independent variables X_i and X_j at the first order.
ε represents the model's error term.

Batch Adsorption Study

The dye degradation efficiency on CFG nanocomposites was conducted by batch adsorption experiments. According to the RSM-BBD design, 27 batches of 50 mL dye solutions were prepared in 100 mL Erlenmeyer flasks, each adjusted with the required initial dye concentration, catalyst dosage, and pH. The prepared samples were exposed to visible light in a designated chamber. Upon completion of the degradation process, the solutions were centrifuged to recover the catalyst, and UV–Vis spectroscopy was used to evaluate the leftover dye concentration. The percentage degradation or removal (η) of the catalyst was determined using the following eqn.-2.[19]

$$\eta = \frac{C_0 - C}{C_0} \times 100 \qquad (2)$$

Where C_0 initial conc of dye and C Conc of dye after photo degradation.

RESULTS AND DISCUSSION

RSM - BBD Analysis

After selecting the appropriate variables, the BBD technique was applied for the optimization of the percentage degradation of Indigo carmine (IC), Eosin Blue (EB) under the conditions of pH (X_1), Catalyst dosage (X_2), Dye concentration (X_3), and Irradiation Time (X_4). Based on coded values, each independent variable is stratified into three levels for analysis: low (-1), medium (0), and high (+1). (Table-1). The percentage of degradation was taken into consideration as the response surface to the variables in the specified experiment, which consisted of 27 distinct experiments. In Table-2, the results of the conducted experiments using BBD, along with the obtained degradation percentages and predicted percentages, are presented.

Table-1: Process Variable Codes and their Levels for the Degradation of Dye

Process variable	Variable Code	Levels		
		-1	0	1
pH	X_1	4	8	12
Catalyst dosage (mg/L)	X_2	25	50	75
Dye concentration (mg/L)	X_3	2	4	6
Irradiation Time (min)	X_4	30	75	120

Table-2: The Four-Factor BBD Matrix and Experimental Results for IC and EB

Run	X_1	X_2	X_3	X_4	% Degradation of IC		% Degradation of EB	
					Actual values	Predicted values (Y)	Actual values	Predicted values (Y)
1	8	75	6	75	58.78	60.24	53.54	53.78
2	8	25	4	120	60.11	75.63	61.94	61.67
3	8	75	4	120	82.1	82.42	65.15	64.94
4	12	50	4	30	17.46	18.65	76.11	75.39
5	8	50	2	120	87.56	85.22	41.25	39.44
6	4	50	4	120	79.11	73.06	36.27	36.19
7	4	25	4	75	54.34	53.67	80.66	80.26
8	12	50	2	75	65.36	63.66	69.33	70.67
9	8	25	2	75	68.96	65.82	35.16	35.01
10	8	50	6	120	75.23	72.84	43.56	44.68
11	8	75	2	75	79.01	72.61	73.21	73.16
12	8	50	4	75	62.05	63.03	80.61	81.83
13	8	25	4	30	19.07	20.81	59.06	58.99

14	12	50	4	120	78.51	73.46	69.45	71.26
15	12	75	4	75	54.35	60.86	53.15	52.4
16	8	50	2	30	32.15	30.4	63.88	65.01
17	8	25	6	75	58.05	53.45	61.99	62.61
18	8	50	4	75	62.05	63.03	71.46	71.31
19	8	75	4	30	25.81	27.6	56.15	55.72
20	12	50	6	75	52.45	51.28	66.55	65.36
21	4	50	2	75	59.96	63.26	33.16	34.35
22	4	50	4	30	18.07	18.25	41.91	41.67
23	4	50	6	75	53.05	50.88	67.21	66.88
24	8	50	6	30	21.17	18.02	86.2	84.44
25	8	50	4	75	62.05	63.03	62.11	62.11
26	12	25	4	75	53.84	54.07	62.11	62.11
27	4	75	4	75	55.05	60.46	62.11	62.11

Model Estimation

The experimental analysis, graph plotting, and coefficient determination were performed using Design Expert (Version 13). Although the cubic model showed higher R^2 values, it was aliased and couldn't differentiate variables. Therefore, the quadratic model, with better R^2 and adjusted R^2 than the linear model, was recommended and selected for accurately fitting the experimental data (Table-3). The ANOVA results for the chosen quadratic model, corresponding to both pollutants, are summarized in Table 4. For Indigo Carmine, the significant model terms were X_2, X_3, X_4, $X_1 \cdot X_1$, and $X_4 \cdot X_4$, with a Predicted R^2 of 0.8440 closely matching the Adjusted R^2 of 0.9413, indicating good model reliability. Similarly, for Eosin Blue, significant terms included X_1, X_2, X_3, X_4, $X_2 \cdot X_4$, $X_3 \cdot X_4$, $X_1 \cdot X_1$, and $X_4 \cdot X_4$, with a Predicted R^2 of 0.9781 aligning well with the Adjusted R^2 of 0.9918, confirming strong model performance. By retaining only the significant terms and eliminating the non-significant ones, the models for both IC and EB degradation were further enhanced. The final models, defining the relationship between pH (X_1), catalyst dose (X_2), dye concentration (X_3), and radiation time (X_4), are presented in Eqn (3) for IC and Eqn (4**)** for EB degradation.

$$\%\text{Degradation of IC} = 62.05 + 0.20X_1 + 3.4X_2 - 6.19X_3 + 27.41X_4 - 0.0511X_1X_2 - 1.5X_1X_3 - 2.33X_2X_3 + 3.81X_2X_4 - 0.3367X_3X_4 - 5.40X_1X_1 - 1.91X_2X_2 + 3.37X_3X_3 - 11.05X_4X_4 \quad (3)$$

$$\%\text{Degradation of IC} = 62.11 + 4.59X_1 + 6.22X_2 - 3.21X_3 + 18.83X_4 + 0.6367X_1X_2 + 0.2337X_1X_3 - 0.25X_1X_4 + 0.084X_2X_3 + 2.56X_2X_4 - 1.59X_3X_4 + 1.83X_1X_1 - 0.0015X_2X_2 - 0.1984X_3X_3 - 5.28X_4X_4 \quad (4)$$

Table-3: Statistical Summary of the Model for Indigo Carmine (IC) & Eosin Blue (EB)

Source	Sequential p-value		Adjusted R^2		Predicted R^2		
	IC	EB	IC	EB	IC	EB	
Linear	< 0.0001	< 0.0001	0.8481	0.9361	0.8033	0.9155	
2FI	0.9786	0.8648	0.8043	0.9237	0.6238	0.8461	
Quadratic	0.0007	< 0.0001	0.9413	0.9918	0.8440	0.9781	Suggested
Cubic	0.5535	0.1922	0.9401	0.9959	-0.3281	0.9100	Aliased

Influence of pH and Exposure Duration on the Degradation of Pollutants

Figures-1 and 2 show that the degradation of IC and EB decreased at lower pH and shorter irradiation times. Since CFG has a pHzpc of 6.2, it becomes negatively charged at pH > pHzpc, enhancing attraction with cationic forms of IC and EB under alkaline conditions, thus improving degradation. Additionally, increased irradiation time sustained photo catalyst activity, enhancing electron-hole generation and ROS production, which boosted degradation efficiency.

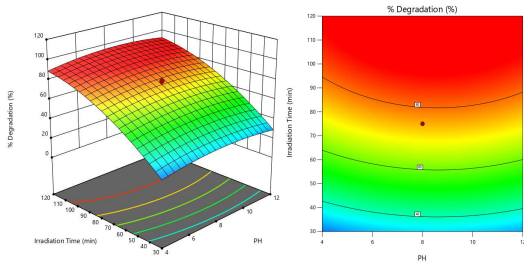

Fig.-1: Degradation as pH and Irradiation Time

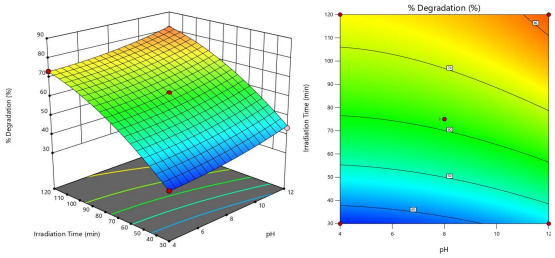

Fig.-2: Degradation as pH and Irradiation Time

Effects of Catalyst Dosage and IC & EB Concentration on Degradation

Effects of varying catalyst dosage and dye concentration, presented in Fig.-3 and 4, show that maximum degradation of IC and EB occurred at 66.32 mg/L and 64.54 mg/L catalyst doses, respectively. Higher catalyst doses increase active sites, enhancing degradation, but excessive amounts lead to particle aggregation, reducing efficiency. Optimal degradation is achieved with balanced catalyst dosage and dye concentration to prevent catalyst saturation, aggregation, or light scattering.

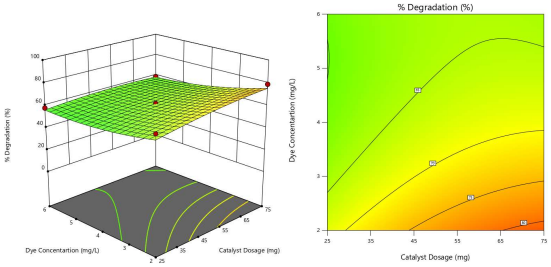

Fig.-3: Degradation as a Function of Dye Concentration and Catalyst Dosage.

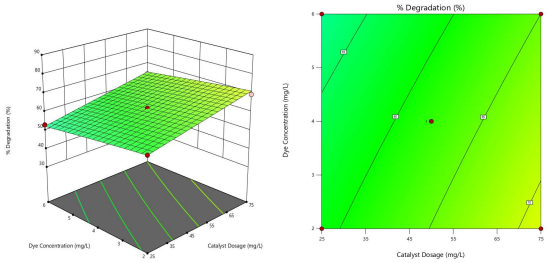

Fig.-4: degradation as Dye Concentration and Catalyst Dosage.

Effect of Catalyst Dosage and Irradiation Time

Figures-5 and 6 illustrate how the catalyst dose and irradiation time influence IC & EB degradation. The slight curvature of the response surface suggests minimal interaction between these factors. Degradation increases significantly with contact time (30–120 min), likely due to rapid adsorption kinetics. Optimal degradation requires balancing catalyst dosage and irradiation time, as excess amounts can cause inefficiencies like catalyst aggregation or energy wastage.

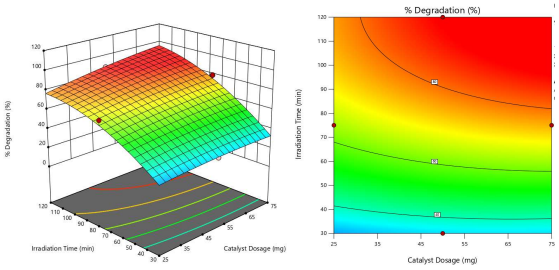

Fig.-5: Degradation as Catalyst Dosage and Irradiation Time

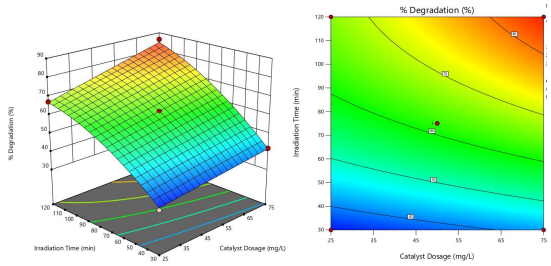

Fig.-6: Degradation as Catalyst Dosage and Irradiation Time

Effect of Concentration of Dye and Irradiation Time

Figures-7 and 8 show that the concentration of dye and the Time of irradiation are key factors in the photocatalytic degradation of IC & EB. High dye concentrations can hinder degradation by saturating the catalyst and reducing light penetration, while prolonged irradiation generally improves degradation but may plateau. Balancing these parameters is crucial for optimization.

Relationship between Actual and Predicted

The actual and predicted responses (Fig.-9) were evenly distributed around the straight line, indicating a strong positive correlation. The close agreement between predicted and adjusted R^2 values further

confirmed the model's reliability, with values of 0.9781 and 0.9918 for Eosin Blue, and 0.8440 and 0.9413 for Indigo Carmine.

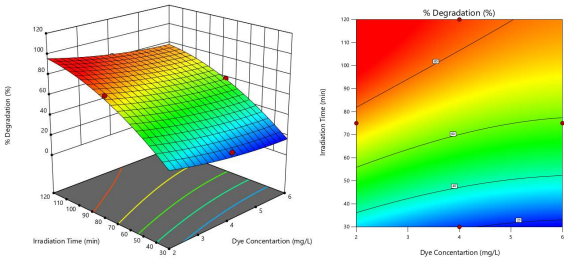

Fig.-7: Degradation as Dye Concentration and Irradiation Time.

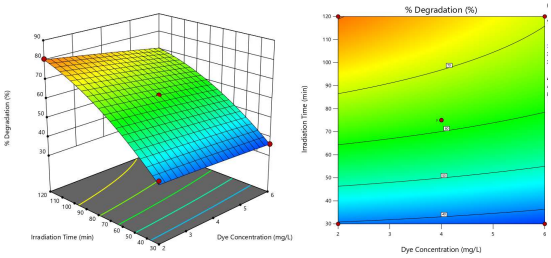

Fig.-8: Degradation as Dye Concentration and Irradiation Time

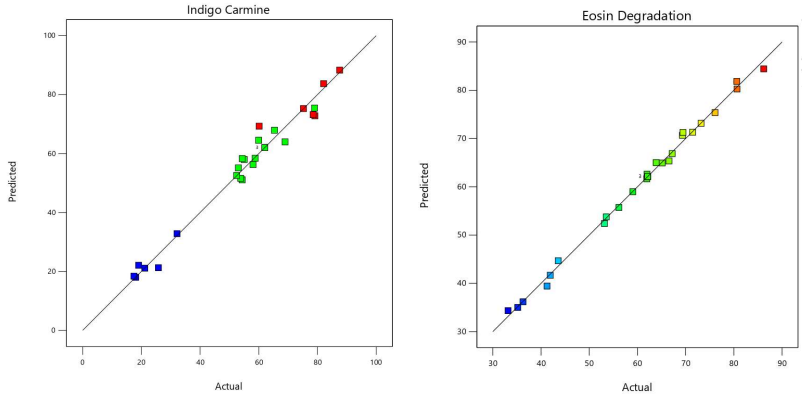

Fig.-9: Relationship between Actual and Predicted % Degradation for the Removal of IC & EB

Optimization and Validation of the Model

The primary objective of the optimization process is to identify the optimal levels of the independent variables. In this study, numerical optimization was performed by adjusting pH, catalyst dosage, dye concentration, and irradiation time within defined limits to achieve the highest degradation efficiency. The resulting optimal values are summarized in Table-5.

Table-4: Analysis of Variance (ANOVA) of the Selected Quadratic Model

Source	Indigo carmine dye					Eosin Blue dye				
	Sum of Squares	df	Mean Square	F-value	p-value	Sum of Squares	df	Mean Square	F-value	p-value
Model	10733.02	14	766.64	30.80	< 0.0001	5364.08	14	383.15	224.79	< 0.0001
X_1	0.4818	1	0.4818	0.0194	0.8917	252.28	1	252.28	148.01	< 0.0001
X_2	138.34	1	138.34	5.56	0.0362	464.31	1	464.31	272.41	< 0.0001
X_3	459.49	1	459.49	18.46	0.0010	123.77	1	123.77	72.62	< 0.0001
X_4	9015.31	1	9015.31	362.21	< 0.0001	4253.05	1	4253.05	2495.24	< 0.0001
$X_1.X_2$	0.0104	1	0.0104	0.0004	0.9840	1.62	1	1.62	0.9515	0.3486
$X_1.X_3$	9.00	1	9.00	0.3616	0.5588	0.2185	1	0.2185	0.1282	0.7266
$X_1.X_4$	0.0000	1	0.0000	0.0000	1.0000	0.2500	1	0.2500	0.1467	0.7084
$X_2.X_3$	21.69	1	21.69	0.8716	0.3689	0.0282	1	0.0282	0.0166	0.8997
$X_2.X_4$	58.06	1	58.06	2.33	0.1526	26.21	1	26.21	15.38	0.0020
$X_3.X_4$	0.4534	1	0.4534	0.0182	0.8949	10.07	1	10.07	5.91	0.0317
$X_1.X_1$	155.38	1	155.38	6.24	0.0280	17.90	1	17.90	10.50	0.0071
$X_2.X_2$	19.41	1	19.41	0.7797	0.3946	0.0000	1	0.0000	7.317E-06	0.9979
$X_3.X_3$	60.67	1	60.67	2.44	0.1444	0.2099	1	0.2099	0.1231	0.7318
$X_4.X_4$	650.77	1	650.77	26.15	0.0003	148.55	1	148.55	87.15	< 0.0001
Residual	298.68	12	24.89			20.45	12	1.70		

Lack of Fit	298.68	10	29.87			20.45	10	2.05		
Pure Error	0.0000	2	0.0000			0.0000	2	0.0000		
Cor Total	11031.70	26				5384.54	26			

(df: degrees of freedom)
* $p < 0.01$ indicates high significance, 0.01–0.05 is significant, and $p > 0.05$ is not significant.

Table-5: Optimum Variables for Degradation of Pollutants

Pollutant	Variables				% Degradation	
	X_1	X_2	X_3	X_4	Experimental	Predicted
Eosin Blue	9.8	64.542	3.985	120	83.554	86.226
Indigo Carmine	8.7	66.329	3.128	120	87.261	88.315

CONCLUSION

In this study, the CFG nanocomposite was used with Box-Behnken Design (BBD) to model and optimize dye degradation. The statistical approach effectively predicted interactions among variables while reducing experimental runs. Results showed CFG's excellent potential in removing Indigo Carmine and Eosin Blue. Future studies could integrate Artificial Neural Networks (ANN) for improved modeling, offering more accurate predictions and deeper insights into degradation mechanisms with minimal experimentation. This work contributes to SDG 6 (Clean Water and Sanitation) by promoting efficient wastewater treatment technologies and SDG 12 (Responsible Consumption and Production) through the development of sustainable, resource-efficient degradation processes.

ACKNOWLEDGMENTS

For their assistance, the authors are deeply grateful to Raghu Engineering College and to the facilities provided by Andhra University's Department of Engineering Chemistry. Special thanks are due to the REC Chemistry Department Head and colleagues for their technical support, talks, and direction during the work.

CONFLICT OF INTERESTS

No conflicts of interest are disclosed by the authors.

AUTHOR CONTRIBUTIONS

The present work is related to *SDG-6: Clean Water and Sanitation*. All the authors contributed significantly to this manuscript, participated in reviewing/editing and approved the final draft for publication. The research profile of the authors can be verified from their ORCID ids, given below:

K. Satyam Naidu https://orcid.org/0000-0003-4985-9206
Nowduri Annapurna https://orcid.org/0000-0003-4946-5362
R. S. K. Sharma https://orcid.org/0000-0001-9338-8208
G. V. Siva Prasad https://orcid.org/0009-0004-8693-4185

REFERENCES

1. A. Demirbas, *Journal of Hazardous Materials*, **157(2)**, 220(2008), https://doi.org/10.1016/j.jhazmat.2008.01.024
2. A. Demirbas, *Journal of Hazardous Materials*, **167(1)**, 1(2009), https://doi.org/10.1016/j.jhazmat.2008.12.114
3. S. Golmohammadi, M. Ahmadpour, A. Mohammadi, A. Alinejad, N. Mirzaei, M. Ghaderpoori, A. Ghaderpoori, *Environmental Health Engineering and Management*, **3(2)**, 107(2016), https://doi.org/10.15171/EHEM.2016.08

4. B. Kamarehie, A. Jafari, M. Ghaderpoori, M.A. Karami, K. Mousavi, A. Ghaderpoury, *Chemical Engineering Communications,* **206(7),** 898(2019), https://doi.org/10.1080/00986445.2018.1537266
5. M. Massoudinejad, M. Ghaderpoori, M. Rezazadeh Azari, *International Journal of Advanced Science and Technology*, **76**, 35(2015), https://doi.org/10.14257/ijast.2015.76.05
6. M. Massoudinejad, M. Ghaderpoori, A. Shahsavani, M.M. Amini, *Journal of Molecular Liquids*, **221**, 279(2016), https://doi.org/10.1016/j.molliq.2016.05.087
7. S. Chakraborty, S. Chowdhury, P.D. Saha, *Carbohydrate Polymers*, **86(4),** 1533(2011), https://doi.org/10.1016/j.carbpol.2011.06.058
8. S. Chakraborty, S. Chowdhury, P.D. Saha, *Clean Technologies and Environmental Policy*, **15(2),** 255(2013), https://doi.org/10.1007/s10098-012-0503-4
9. M. Rafatullah, O. Sulaiman, R. Hashim, A. Ahmad, *Journal of Hazardous Materials*, **177(1),** 70(2010), https://doi.org/10.1016/j.jhazmat.2009.12.047
10. *Global NEST Journal*, (2020), https://doi.org/10.30955/gnj.003089
11. B. Gözmen, M. Turabik, A. Hesenov, *Journal of Hazardous Materials*, **164(2),** 1487(2009), https://doi.org/10.1016/j.jhazmat.2008.09.075
12. Z. Belala, M. Jeguirim, M. Belhachemi, F. Addoun, G. Trouvé, *Desalination*, **271(1)**, 80(2011), https://doi.org/10.1016/j.desal.2010.12.009
13. B. Noroozi, G.A. Sorial, H. Bahrami, M. Arami, *Journal of Hazardous Materials*, **139 (1)**, 167(2007), https://doi.org/10.1016/j.jhazmat.2006.06.021
14. A. Asfaram, M. Ghaedi, G.R. Ghezelbash, E. Alipanahpour Dil, I. Tyagi, S. Agarwal, V.K Gupta, *Journal of Molecular Liquids*, **214,** 249 (2016), https://doi.org/10.1016/j.molliq.2015.12.075.
15. V.K. Gupta, Suhas, *Journal of Environmental Management*, **90(8),** 2313(2009), https://doi.org/10.1016/j.jenvman.2008.11.017
16. P. Saha, S. Chowdhury, S. Gupta, I. Kumar, R. Kumar, *CLEAN Soil, Air, Water* **38(5)**, 437(2010), https://doi.org/10.1002/clen.200900234
17. M.A.M. Salleh, D.K. Mahmoud, W.A.W. Abdul Karim, A. Idris, *Desalination,* **280(1)**, 1(2011), https://doi.org/10.1016/j.desal.2011.07.019
18. G.O. El-Sayed, *Desalination*, **272(1)**, 225(2011), https://doi.org/10.1016/j.desal.2011.01.025.
19. U.K.Sahu, S.S.Mahapatra, R.K.Patel, *Materials Chemistry and Physics*, **207**, 233(2018), https://doi.org/10.1016/j.matchemphys.2017.11.042
20. A. Gomathi, T. Prabhuraj, S. Gokilapriya, G. Vasanthi, P. Maadeswaran, K.A. Ramesh Kumar, *Dyes and Pigments*, **218**, 111473(2023), https://doi.org/10.1016/j.dyepig.2023.111473

[RJC-9317/2025]